

1 **The impact of land cover generated by a dynamic**  
2 **vegetation model on climate over East Asia in present and**  
3 **possible future climate**

4  
5 **Mee-Hyun Cho<sup>1</sup>, Kyung-On Boo<sup>2</sup>, G. M. Martin<sup>3</sup>, Johan Lee<sup>2</sup>, Gyu-Ho Lim<sup>1</sup>**

6  
7 [1]{School of Earth and Environmental Sciences, Seoul National University, Seoul, Republic  
8 of Korea}

9 [2] {National Institute of Meteorological Research, Korea Meteorological Administration,  
10 Seoul, Republic of Korea}

11 [3] {Met Office Hadley Centre, FitzRoy Road, Exeter, UK}

12 Correspondence to: M.-H. Cho (mhjo77@snu.ac.kr)

13  
14 **Abstract**

15 This study investigates the impacts of land cover change, as simulated by a dynamic vegetation  
16 model, on the summertime climatology over Asia. The climate model used in this study has  
17 systematic biases of underestimated rainfall around Korea and overestimation over the South  
18 China Sea. When coupled to a dynamic vegetation model, the resulting change in land cover is  
19 accompanied by an additional direct radiative effect over dust-producing regions. Both the  
20 change in land surface conditions directly and the effect of increased bare soil fraction on dust  
21 loading, affect the climate in the region, and are examined separately in this study. The direct  
22 radiative effect of the additional dust contributes to increasing the rainfall biases, while the land  
23 surface physical processes are related to local temperature biases such as warm biases over

24 North China. In time-slice runs for future climate, as the dust loading changes, anomalous  
25 anticyclonic flows are simulated over South China Sea, resulting in reduced rainfall over the  
26 South China Sea and more rainfall near Korea and South China. In contrast with the rainfall  
27 changes, the influence of land cover change and the associated dust radiative effects are very  
28 small for future projection of temperature, which is dominated by atmospheric CO<sub>2</sub> increase.  
29 The results in this study suggest that the land cover simulated by a dynamic vegetation model  
30 can affect, and be affected by, model systematic biases on regional scales over dust emission  
31 source regions such as Asia. In particular, analysis of the radiative effects of dust changes  
32 associated with land cover change is important in order to understand future changes of  
33 regional precipitation in global warming.

34

## 35 **1 Introduction**

36 Bordered by the Tibetan Plateau to the west, the Eurasian land mass to the northwest, and the  
37 vast Pacific Ocean to the south and east, East Asia has experienced one of the most pronounced  
38 monsoon climates of the globe for centuries (Lau and Li, 1984). Land surface properties are  
39 important because of their known impact on the East Asian monsoon circulation (Kang and  
40 Hong, 2008; Lee et al., 2011) and on the Indian monsoon (Douglas et al., 2006; Lee et al., 2009;  
41 Battle Bayer et al., 2012; Martin and Levine, 2012). Lee et al. (2011) proposed that a  
42 replacement of vegetation with bare soil would cause an associated decrease in latent heat  
43 during the summer, which could weaken East Asian monsoon circulation. This decrease in  
44 latent heat flux over land could weaken the East Asian monsoon via a positive feedback  
45 between the latent heat flux contrast and rainfall. Yamashima et al. (2011) showed a similar  
46 study over the Indian subcontinent and Southeastern China. Land surface property changes  
47 from forest to cultivated land have resulted in a decrease in the monsoon rainfall and provoked  
48 an associated weakening of the Asian summer monsoon circulation. Moreover, there are a few  
49 studies investigating the influence of land cover change that have demonstrated significant  
50 impact on East Asian Monsoon (Kang et al., 2005), but they usually used satellite-based (Suh  
51 and Lee, 2004; Kang and Hong, 2008) and idealized land cover change (Lee et al., 2011).

52 Although Earth System models with dynamic vegetation schemes allow representation of the  
53 carbon cycle feedbacks on climate, the land cover distribution could also be influenced by, and  
54 indeed influence, model systematic biases (Martin and Levine, 2012, hereafter ML12). Land  
55 surface property changes have effects on the atmosphere through physical processes (such as  
56 changes in surface roughness, albedo and evapotranspiration), and can induce additional  
57 indirect impacts when coupled with aerosol processes as well. For example, changes in surface  
58 emissions of mineral dust that are caused by changes in bare soil fraction will have a radiative  
59 effect in the atmosphere. Additional dust loading of the atmosphere resulting from land cover  
60 change in an Earth System model could, therefore, add to the model uncertainty via feedbacks  
61 with model systematic biases such as lack of rainfall over dust-producing regions. Dust affects  
62 both shortwave and longwave radiative fluxes, and the effects of mineral dust on the radiation  
63 budget are important due to the widespread distribution and large optical depth of mineral dust  
64 (Sokolik and Toon, 1996). A study by Yoshioka et al. (2007) suggests that the direct radiative  
65 forcing of dust can explain up to 30% of the observed precipitation reduction in the Sahel in  
66 **30 year simulation**. Dust is removed from the atmosphere by both dry and wet deposition  
67 processes, providing a source of iron to phytoplankton and thus potentially affecting the carbon  
68 cycle (Collins et al., 2011). Since Northeast Asia is one of the major dust emission source  
69 regions, land surface property changes over this source region need to be studied. Aerosol, as  
70 one of the fundamental atmospheric constituents, has an important impact on the climate  
71 system. Ramanathan et al. (2005) showed that global dimming causes a long-term (multi-  
72 decadal) weakening of the South Asian monsoon by reducing the meridional surface  
73 temperature gradient between the Asian land mass and the Indian Ocean. Aerosol affects  
74 precipitation events through cloud physics processes in China (Qian et al., 2009), while dust  
75 can also contribute to Asian monsoon rainfall anomalies by heating the upper troposphere (Lau  
76 et al., 2006, Lau and Kim, 2006). Therefore, aerosol impacts due to land cover changes may  
77 be important in regional climate over East Asia.

78 ML12 investigated the impacts on climate of land cover changes, and associated dust effects,  
79 that resulted from model systematic biases. Their results reflect that over dust producing  
80 regions, land cover change simulated by a Dynamic Global Vegetation Model (DGVM) can  
81 affect both the present-day simulation and the future response as well. According to Hurrell et

82 al. (2009) and McCarthy et al. (2012), since model systematic biases affect climate model  
83 sensitivity, we need to study processes related to systematic biases in order to understand future  
84 climate projections. Motivated by ML12, this study extends ML12 by applying their results for  
85 East Asia. The aims of this study are: first, to investigate the physical influence of changes in  
86 land cover conditions and associated changes in aerosol loading on the rainfall and surface  
87 temperature over East Asia; and second, to provide insight into the possible conflicting  
88 contributions to uncertainty in climate projections for the region that come from the inclusion  
89 of dynamic vegetation in a climate model (which ought to be beneficial) and its interaction  
90 with existing precipitation biases (which is detrimental).

91 The present paper is organized as follows. Section 2 briefly describes the global circulation  
92 model used in this study, the experimental design, and the data. The results of the study are  
93 given in section 3. The impact of land cover distribution and radiative effect of dust under  
94 present and possible future climate are all provided in this section. A summary and discussion  
95 are given in section 4.

96

## 97 **2 Model Experimental Design and Data**

98 In this study, we used the same datasets as used in ML12, and we follow a similar methodology  
99 for the analysis, with additional investigation of particular aspects concerning the East Asian  
100 region. The experiments were produced using the Hadley Centre Global Environmental Model  
101 version 2 (HadGEM2) model family that had been developed by the UK Met Office (The  
102 HadGEM2 Development Team, 2011). The horizontal grid interval was  $1.25^\circ \times 1.875^\circ$  in the  
103 latitude-longitude directions, and 38 vertical layers were used with the top of atmosphere over  
104 39 km in height. The land surface scheme in the HadGEM2 family is a tiled version of the Met  
105 Office Surface Exchange Scheme (MOSES) version 2, which represents heterogeneous surface  
106 properties (Cox et al., 1999; Essery and Clark, 2003). A grid box represents a mixture of five  
107 vegetation or plant-functional types (PFTs), which include broadleaf trees, needleleaf trees,  
108 temperate C<sub>3</sub> grass, tropical C<sub>4</sub> grass, and shrubs, and four non-vegetated surface types, which  
109 include urban, inland water, bare soil, and ice. Surface fluxes and temperatures are calculated

110 separately for each surface type and are aggregated according to each tile's fractional coverage  
111 before being passed to the atmospheric model (Lawrence and Slingo, 2004).

112 The experiment configuration used by ML12 is as follows. For the present-day (1980-2005)  
113 runs, the HadGEM2 atmosphere-only model was forced with observed sea surface  
114 temperatures (SSTs) and sea ice. The experimental design and forcing datasets are as specified  
115 by the Fifth Coupled Model Intercomparison Project (CMIP5; Taylor et al., 2012) and are  
116 detailed in Taylor et al. (2012). The land cover and vegetation types were prescribed by the  
117 International Geophysical Biophysical Programme (IGBP; Loveland et al., 2000) with a  
118 prescribed seasonally-varying leaf area index (LAI) based on Moderate Resolution Imaging  
119 Spectroradiometer (MODIS) Terra Collection 5 monthly LAI datasets. Historical land use  
120 change information based on CMIP5, provided to CMIP5 by the Land Use Harmonization team  
121 (Hurtt et al., 2011), were applied by Baek et al. (2013) to the IGBP land cover data in order to  
122 prescribe time-varying land cover fields for HadGEM2-A. This is referred to as the "A"  
123 experiment.

124 For the future timeslice experiments, the atmosphere component is forced with CO<sub>2</sub> and trace  
125 gases for the year 2100 based on the Representative Concentration Pathway (RCP) 8.5 scenario  
126 of the CMIP5 (Taylor et al., 2012). The SSTs were obtained by applying the difference between  
127 30-year mean SSTs centred around 2100 (from the HadGEM2 Earth System (HadGEM2-ES)  
128 RCP8.5 scenario coupled model run) and 30-years mean SSTs centred around 1990 (from the  
129 HadGEM2-ES historical run), to the present-day monthly-varying observed SSTs from 1980–  
130 2005. The projected future land use changes for the period 2080-2110 based on CMIP5 RCP8.5  
131 scenarios were applied in order to prescribe time-varying land cover fields (Hurtt et al., 2011)  
132 for HadGEM2-A timeslice experiment. This is referred to as the "Ats" experiment.

133 In addition to the "A" and "Ats" experiments, alternative representations of global vegetation  
134 cover from a DGVM were used as the land cover component for further HadGEM2-A  
135 experiments under present-day and future climates. In these experiments, the only change made  
136 is that the monthly mean land cover information from the HadGEM2-ES historical and RCP8.5  
137 runs is used in HadGEM2-A in place of the standard land cover distribution as described above.  
138 **The HadGEM2-ES configuration uses the Top-down Representation of Interactive Foliage and**

139 **Flora Including Dynamics (TRIFFID) dynamic vegetation model (Cox, 2001) to simulate the**  
140 **land cover changes.** Therefore, in these additional experiments, the variations in land cover  
141 with time during these periods in HadGEM2-ES are experienced by HadGEM2-A, but there is  
142 no interactive terrestrial carbon cycle and no feedbacks on the land cover. Variations in land  
143 cover from years 1980–2005 of HadGEM2-ES are used in the present-day experiment of this  
144 type, referred to as “AE”, while the variations in land cover from years 2080-2110 of  
145 HadGEM2-ES are applied to the future timeslice experiment denoted “AEts”. Note that crops  
146 are not represented explicitly in HadGEM2-ES; crop and pasture are assumed to be a  
147 combination of C<sub>3</sub> and C<sub>4</sub> grass. Details of how land use changes relating to cropland are  
148 applied in HadGEM2-ES are given in Jones et al. (2011). This simplification could affect the  
149 sensitivity to land cover changes in East Asia in our experiments.

150 A mineral dust scheme (Woodward, 2011) is included in the HadGEM2 model family  
151 (HadGEM2 Development Team, 2011) which permits the simulation of changes in mineral  
152 dust concentration in response to changes in surface conditions as well as its interaction with  
153 model climate via radiative effects. According to ML12, the AE experiment shows a large  
154 increase in dust, which is generated as a result of the feedback between the interactive  
155 vegetation and the model's systematic rainfall biases in dust-producing regions. Dust is only  
156 emitted from the bare soil fraction of a grid-box, and therefore is sensitive to changes to this  
157 fraction when the DGVM is used. **In the model, the dust affects both shortwave and longwave**  
158 **radiative fluxes. The semi-direct effect is included implicitly with absorption by the dust**  
159 **feeding back onto the atmospheric heating profiles and subsequently cloud distributions, but**  
160 **the dust is not microphysically active.** To evaluate the radiative effects of the dust, an additional  
161 pair of experiments was carried out where the direct radiative effects of the dust were switched  
162 off. This reduces the dust to a passive tracer in the model with no feedback on the climate.  
163 These experiments have the suffix “nod” meaning “no dust radiative effects”. Therefore,  
164 “Anod” means a HadGEM2-A simulation with the standard land cover distribution in the  
165 present-day, “AEnod” means a HadGEM2-A present-day simulation with HadGEM2-ES land  
166 cover without the direct radiative effects of the dust, and “AEnodts” means a HadGEM2-A  
167 future timeslice simulation with HadGEM2-ES land cover without the direct radiative effects  
168 of dust. The total experiments are listed in Table 1.

169 To compare model results in the present-day runs with observations we used the Global  
170 Precipitation Climatology Project (GPCP) precipitation (Alder et al., 2003; Huffman et al.,  
171 2009), the CPC Merged Analysis of Precipitation (CMAP, Xie and Arkin, 1997) and the  
172 Climatic Research Unit (CRU) mean surface air temperature (Harris et al., 2013). In this study,  
173 summer represents the period from June to August.

174

### 175 **3 Modeling Results**

176

#### 177 **3.1 Present Day**

##### 178 **3.1.1 Impact of ES land Cover on Average Temperature and Precipitations**

179

180 First we examine summer precipitation over East Asia. Figure 1a shows the climatological  
181 summertime precipitation distribution of the East Asian summer monsoon. The summer  
182 monsoon rainy season evolves with the rainband development covering South China, Korea,  
183 Japan and the adjacent seas. Formation of frontal systems is associated with the North Pacific  
184 Subtropical High and southwesterlies over the South China Sea. The rainband region, in  
185 contrast with the equatorial region, has a small observational uncertainty (Fig. 1b). In Fig. 2,  
186 we analyze the North China (NC) region (35-50° N, 105-120° E), Korea (KR) 25-40° N, 120-  
187 135° E, and South China (SC) region (20-35° N, 105-120° E), which together represent a large  
188 contrast in land cover distribution over East Asia. Simulated precipitation compared with  
189 observation (GPCP precipitation) shows a systematic bias in Fig. 2. Precipitation is  
190 underestimated over the KR area and overestimated over SC. These spatial features remain in  
191 AE, although the underestimated rainfall over KR become larger in AE than A.

192 Figure 3 represents summer surface air temperature bias in the model results compared with  
193 the CRU observation data. There is a warm bias greater than 1K in NC and KR, but only a  
194 small bias in SC (Fig. 3a). The warm bias over KR is slightly smaller in AE compared to A

195 (Fig. 3c, d). In order to shed light on the bias changes on the regional scale, the land cover  
196 difference between AE and A is examined (Fig. 4). Among the five vegetation and bare soil  
197 surface types over East Asia, the largest changes are in broadleaf, C<sub>3</sub> grass and bare soil types.  
198 Over North China, the increase in bare soil fraction is large. This unrealistic high bare soil  
199 fraction has an impact on high dust emission over this region because dust is only emitted from  
200 the bare soil fraction of a grid box in this model. In contrast, the South China region is covered  
201 by larger broadleaf fraction (Fig. 4) in the AE compared with A, replacing bare soil, shrub and  
202 needle-leaf tree. To the north of 50°N, the increase in shrub fraction is distinct (also seen in Fig.  
203 4 of ML12).

204 ML12 showed that bare soil area expansion from the changes in the vegetation distribution  
205 between AE and A generates additional dust, resulting in a substantial direct radiative impact  
206 on the Indian monsoon rainfall. They suggest separate analysis for the dust radiative feedback  
207 resulting from land cover change from the analysis of the effects of the change in surface  
208 conditions. Accordingly, we examine experiments Anod and AEnod (see Table 1).

209 In Fig. 2, a marked precipitation underestimation over KR is shown compared with  
210 observations, particularly when the ES land cover is used. The dry bias amplitudes in summer  
211 become larger in AE compared with A (Fig. 2). To estimate the radiative effect of dust on  
212 rainfall when the HadGEM2-ES land cover distribution was used, AE was compared with  
213 AEnod. The dry bias amplitude of AE decreases in AEnod (Fig. 2c and f) but is still slightly  
214 larger than in A. Thus the radiative effect of dust reinforces the dry bias in the KR region  
215 (compare Fig. 2b and 2e with Fig. 2c and 2f). This is consistent with the results of ML12 for  
216 the South Asian region. ML12 showed significant effects of the change in dust loading on the  
217 clear-sky radiative fluxes across South and East Asia (their Fig. 7) and commented on the  
218 impacts on surface temperatures which tend to reduce precipitation through cooling of the  
219 daytime maxima.

220 To examine the dust radiative effect and land cover change effect in detail, the dry bias in  
221 summer over KR in Fig. 2 is considered using Fig. 5. The pattern of changes between "AE-A"  
222 in Fig. 5a is similar to the "AE – AEnod" changes (Fig. 5c) rather than those of "AEnod –



223 Anod” (Fig. 5b). This suggests that precipitation over East Asia is more sensitive to the  
224 radiative effects of dust associated with land cover changes than to the land cover change alone.

225 In Fig. 6 we make a similar comparison for surface air temperature changes. We find that the  
226 dust radiative effect on surface air temperature is associated with a small widespread cooling  
227 (Fig. 6c), whereas the surface process effects of the land cover change are associated with a  
228 more substantial warming/cooling pattern across the region, as shown in the AEnod-Anod (Fig.  
229 6b) and AE-A (Fig. 6a) differences. Over northeastern Eurasia, the increase of shrub fraction  
230 replacing broadleaf and needleleaf trees shows a distinct cooling of surface air temperature  
231 induced from an increase of surface albedo.

232

### 233 **3.1.2 Impact of Changes in Land Cover with No Dust Radiative Feedback**

234 To understand more clearly the impacts of the changes in the vegetation distribution in Fig. 6a  
235 and 6b, we examined the climate response without the direct radiative effect of dust. The  
236 aforementioned increase in warm bias over NC “AEnod–Anod” (Fig. 6b) is considered. Over  
237 NC, as the bare soil fraction is larger in AE than A (Fig. 4f; Fig. 7ab), the roughness length  
238 reduces while soil evaporation and canopy evaporation decrease. Reduced roughness length  
239 induces a decrease of sensible and latent heat fluxes from the surface to the atmosphere (Fig.  
240 7c, d, f). The decrease in latent heat flux is associated with reduced cloud amount (Fig. 7e), as  
241 well as being favorable for surface warming. As a result, surface air temperature rises over NC  
242 (Fig. 7h). The reduced latent heat flux is particularly evident in the canopy evaporation in the  
243 NC region, although there is also reduced soil evaporation during the summer (not shown).

244 Similarly, surface cooling over SC and KR is considered in summer. Broadleaf tree fraction  
245 expansion (Fig.7b) increases the roughness length (Fig. 7f) and latent heat flux (Fig. 7c),  
246 driving surface cooling. While the NC region, where bare soil fraction is increased, showed a  
247 decrease of evaporation from A to AE, in the KR and SC regions where broadleaf tree fraction  
248 is increased there is increased soil and canopy evaporation from A to AE. These results are  
249 consistent with the suggestion by Lee et al (2011) that a vegetation replacement with bare soil  
250 would cause an associated decrease in latent heat during the summer. In summary, for the

251 present climate, the land cover effect (bare soil fraction changes in Fig. 7a) is related to surface  
252 air temperature changes in summer (Fig. 7h). As bare soil fraction expands (shrinks) the  
253 temperature rises (drops).

254 As regards precipitation, Fig. 6 shows only very small changes in precipitation over land in  
255 AEnod-Anod (Fig. 6b), and Fig. 10a also shows only small changes in the circulation between  
256 these experiments. Thus, the model's direct sensitivity of precipitation to changes in land  
257 surface conditions seems to be low compared with the sensitivity to the dust changes that result  
258 from them. Although this conclusion is similar to that for India in ML12, the remote influence  
259 of changes in springtime Eurasian snow cover associated with the change in vegetation was  
260 highlighted for South Asia in that study, whereas for the East Asian region we have shown a  
261 more local influence of changes in surface conditions.

262

### 263 **3.1.3 Impact of Dust Radiative Feedback**

264 We now consider the direct radiative effect of dust resulting from the changes in the vegetation  
265 distribution (AEnod-Anod and AE-AEnod of Fig. 8). Concerning the regional climate response,  
266 the dust direct radiative effects (Fig. 8b) lead to anomalous northeasterly coastal flow  
267 counteracting the summertime climatological monsoonal circulation associated with the  
268 western North Pacific high, known to be important in the East Asian summer monsoon rainfall  
269 (Lee et al. (2006) and Fig. 8c). The sea level pressure and wind anomalies in "AE - AEnod"  
270 are stronger than those of "AEnod - Anod" (Fig. 8a and b), illustrating that the radiative effects  
271 of the dust have a larger impact than the surface vegetation changes themselves.

272 The direct radiative effect of dust induces anomalous cyclonic flow over the western North  
273 Pacific (KR region in Fig. 8b) that would tend to decrease rainfall over East Asian continent.  
274 This is because dust reflects a considerable amount of shortwave radiation, as shown by the  
275 increase of upward shortwave radiation at the top of atmosphere (TOA; Fig. 8f), with a  
276 resulting cooling the land surface (Fig. 8d). The land surface cooling appears on the continental  
277 scale. This is somewhat different from the results in Miller and Tegen (1998) in which they  
278 mentioned that the reflected solar flux is offset by the absorption of upwelling longwave

279 radiation, so that the net radiation entering the TOA is only weakly perturbed by dust in  
280 comparison to the surface reduction. Although the upward longwave flux is reduced through  
281 the dust radiative effects (Fig. 8e), the reduction is smaller than the increase in reflected  
282 shortwave at the TOA. Differential heating between land and ocean is one of the fundamental  
283 driving mechanisms of the monsoon (Webster et al., 1998). The land-sea thermal contrast  
284 becomes weaker due to the direct radiative effect of dust and the pressure contrast weakens.  
285 Strong anomalous northeasterly flow along the coast (Fig. 8b), weakening the summer  
286 monsoon inflow, induces the dry bias over SC and KR (Fig. 5c). These results seem in line  
287 with the argument that dust-induced surface cooling is the dominant mechanism leading to a  
288 reduction of precipitation (Konaré et al., 2008; Yoshioka et al., 2007; Paeth and Feichter, 2005).

289

### 290 **3.2 Future experiments**

291 The effect of including a DGVM, particularly with the feedback on the dust loading, is expected  
292 to affect the simulation of future climate change. Changes in AETs relative to AE show  
293 increases in rainfall over SC, KR and the western North Pacific (Fig. 9b). Compared with  
294 differences between A<sub>ts</sub> and A in Fig. 9a, Fig. 9b shows a further reduction in rainfall over the  
295 South China Sea (SCS) to the south of 20°N accompanied by anticyclonic flow at 850hPa. The  
296 discrepancy in future changes in precipitation tends to be larger than that of temperature: Fig.  
297 9c and 9d present similar warming patterns.

298 In order to examine the role of different vegetation distributions in global warming, with and  
299 without the dust feedbacks, we analyze future timeslice experiments in a similar manner to  
300 ML12. To estimate individually the impact of land cover, feedback on the dust loading, and  
301 climate change of global warming, we use the experiments described in Table 2. Note that  
302 “Dust” and “LCC” are ‘double differences’ illustrating the impacts of the inclusion of the land  
303 cover changes, and the radiative effects of the dust changes that the land cover change induces,  
304 on the future-present differences.

305 According to Baek et al (2013), the warming and rainfall increment from RCP8.5 are expected  
306 to be of the order of  $6 \pm 1\text{K}$  and 17% over East Asia. The temperature rises in the timeslice

307 experiments are of similar magnitude (Fig. 9c, 9d, 10b). Consistent with this, Fig. 9 and Fig.  
308 10 project a warmer and wetter climate in future summer over NC, KR and SC. Fig. 9b and  
309 Fig. 10a show that a larger increase in rainfall between future and present timeslice run is  
310 simulated in these regions when land cover change and feedback on the dust are included.  
311 However, while precipitation changes over the SCS region tend to be slightly positive on  
312 average in climate change-only, including land cover changes and feedback with dust induces  
313 a reduction in rainfall in this region.

314 The land surface cover differences in this region between future and present-day climate  
315 projected by this model are in C<sub>3</sub> grass expansion replacing bare soil (Fig. 11c, 11f). These  
316 changes contribute increases in the evaporation and latent heat flux and decreases in surface  
317 air temperature (Fig. 12a, 12b) to the overall future-present changes. Comparison between  
318 (AEnodts - AEnod) and (A<sub>ts</sub>-A) in Fig. 9 showed that the changes in land cover contribute to  
319 increased rainfall over the land and reduced rainfall over the SCS. Increasing latent heat flux  
320 accompanies lower boundary layer height and is associated with boundary layer moistening  
321 (Fig. 12c). According to Lee et al. (2009, 2011), a more vegetated surface tends to be associated  
322 with surface moistening, favoring an increase in latent heat and atmospheric moisture (Fig. 12).  
323 The changes in vegetation and associated changes in surface air temperature, latent heat fluxes  
324 (Fig. 12a and b) and low level circulation (Fig. 12d) are in a similar pattern, but opposite sign,  
325 to those shown in Fig. 7c, 7h and 8a. This suggests that the future differences between  
326 experiments with different land cover (AEnodts - A<sub>ts</sub>) are small compared with the present-  
327 day differences (AEnod-A) such that the double-difference (AEnodts - AEnod) - (A<sub>ts</sub> - A)  
328 is dominated by the present-day differences. This is consistent with the findings of ML12.

329 In Fig. 12d, increased rainfall over the SC region from 25°N to 35°N is associated with  
330 additional anomalous convergence and upward motion over the SC region (see Fig. 13a)  
331 induced by the land cover change effect as the monsoon differential circulation results in  
332 enhanced moisture transport and cloud formation over SC and KR. In contrast, over the SCS,  
333 anomalous anticyclonic flow is related to downward motion from 10°N to 20°N (Fig. 13a) and  
334 reduced rainfall (Fig. 12d). The local influence on rainfall of the changes in surface temperature,  
335 fluxes and low-level circulation related to the changes in land cover over East Asia are in

336 contrast to the larger-scale responses described in ML12 for South Asia, where the role of  
337 future changes in tree cover over northeast Eurasia in the dynamical response associated with  
338 the change in meridional temperature gradient was highlighted.

339 As shown in Fig. 10a, the dust radiative forcing is the main contributor to the reduction of  
340 simulated precipitation over SCS to the south of 20°N in the AETs future experiment. Figure  
341 14 shows the double-difference (AETs minus AE) minus (AENodts minus AENod). The  
342 atmospheric response shown in Fig. 14 seems to be largely opposite to that in Fig. 8b, 8e and  
343 8f, suggesting that it is dominated by the present-day impacts of dust seen between AE and  
344 AENod. In global warming (i.e. future-present), the bare soil fraction decreases (Fig. 11f) so  
345 the dust emission of HadGEM2-ES decreases in the future relative to the present climate  
346 (Fig.15). As mentioned in Section 3.1.3, the direct radiative effect of dust seems to induce  
347 stronger flow than that of ES land cover-only effect. The convective region over SC in the  
348 future experiment Aets (Fig. 9a, 13c) is strengthened in AETs (Fig. 9b), and that over the SCS  
349 weakened, through the radiative effects of the reduced dust loading (Fig. 13b), with related  
350 increases and decreases in precipitation (Fig. 14d and 10a).

351 Overall, for future precipitation projection over East Asia using this model, simulating  
352 interactive land cover change by a DGVM, and particularly the subsequent changes in dust  
353 radiative effect, are at least as important as the warming conditions. In contrast, for future  
354 changes in temperature, the global warming effect is dominant among climate change, land  
355 cover change and dust radiative effects over East Asia (Fig. 9c, 9d and 10b).

356

#### 357 **4 Summary and Discussion**

358 In this study, the impact of varying land cover distribution, as simulated by a DGVM, on  
359 simulated regional climate over East Asia is examined. The interaction between land cover  
360 change by the DGVM and model systematic biases are shown in the present-day climate. The  
361 climatology of HadGEM2-A has an underestimation of rainfall over KR in summer and an  
362 overestimation over SC. When the land cover from HadGEM2-ES, which uses an interactive  
363 vegetation model, is used as an input to HadGEM2-A (experiment AE), the precipitation bias

364 is enhanced over KR and SCS. The difference between AE and A is related to regional bare  
365 soil expansion by the DGVM through interaction with the rainfall bias, and also through  
366 feedback with the subsequent dust loading, causing a direct radiative effect. The direct radiative  
367 effect of dust has an important influence on both the precipitation bias and the stronger  
368 circulation response in SLP and wind than the land cover-only effect does. In this study, more  
369 dust loading due to excessive bare soil fraction induces an amplified dry bias over Asia. The  
370 land cover difference between AE and A affects the surface air temperature bias. In summer, a  
371 warm bias in NC (Fig. 7h) is due to bare soil area expansion replacing vegetation (Fig. 7). Soil  
372 fraction expands (shrinks) and temperature rises (drops) over NC (SC) (Fig. 7) through changes  
373 in surface roughness, evaporation and latent heat fluxes.

374 The dust loading is expected to reduce in the future time-slice run, since C<sub>3</sub> grass replaces bare  
375 soil area over NC. The consequent direct radiative effect of dust changes induces the opposite  
376 direction of anomalous wind flow over the SCS compared with that induced by the CO<sub>2</sub>  
377 increase alone. Thus, in the future projection, suppressed rainfall appears over the SCS. Just as  
378 the direct radiative effect is significant in the future precipitation simulation, the land cover  
379 effect is also important. The C<sub>3</sub> grass expansion replacing bare soil, inducing an increase in  
380 latent heat flux, lowers the surface temperature. The changes in land cover between future and  
381 present day tend to oppose the surface warming over NC and KR in summer that are driven by  
382 increasing CO<sub>2</sub> in the time-slice experiments. When the land cover change impacts and  
383 associated dust radiative effect are combined, the resulting rainfall under future climate differs  
384 regionally. In contrast with the precipitation response, the temperature response in the time-  
385 slice run is dominated by the warming induced from the atmospheric CO<sub>2</sub> increase. In terms of  
386 the projected temperature rise, the ES land cover and dust radiative effects are very small.  
387 Overall, the inclusion of land cover changes as simulated by an interactive vegetation model  
388 has impacts on both present and future climate in East Asia. These results are similar to those  
389 for India shown in ML12, although the response amplitude is different. In addition, local rather  
390 than remote mechanisms appear to influence the precipitation and circulation response in this  
391 region, whereas for India the role of land cover changes in northern Eurasia on the large-scale  
392 meridional temperature gradient was highlighted in ML12.

393 Inclusion of dynamic vegetation components in a climate model allows impacts of climate  
394 change on both atmospheric composition and ecosystems. When the various feedbacks among  
395 the model components are included, complexity increases and the feedbacks affect more  
396 numerous systematic biases in models and future climate projections (ML12). As discussed in  
397 ML12, as additional Earth System processes are included in a model, the complex interactions  
398 and feedbacks between these additional parameterized processes and the model's existing  
399 systematic biases, in e.g. rainfall, can be an additional source of uncertainty in climate  
400 projection. Therefore it is imperative that model developers continue to strive to improve  
401 physical parameterizations in modelling systems. We would emphasize that the details of our  
402 results may be dependent on the particular modelling system used for this study. Experiments  
403 with more subtle or realistic possible land cover changes have not been carried out for this  
404 region with this model, and studies of the influence of vegetation changes using other models  
405 (e.g. Lee et al., 2011) have not examined the feedbacks on dust. Therefore, we are unable to  
406 speculate on the relative importance of the dust feedback effects under more subtle or realistic  
407 possible land cover change scenarios. Nevertheless our results suggest that vegetation  
408 feedbacks may be important over East Asia, particularly in the dust emission source regions,  
409 for present-day and future climate simulation. Thus, we encourage other modelling centres to  
410 investigate these responses in other models where the biases may be different.

411

## 412 **Acknowledgments**

413 This research was supported by the National Institute of Meteorological Research, Korea  
414 Meteorological Administration (project NIMR-2012-B-2), and it used the Unified Model (UM)  
415 licence. G.M. Martin was supported by the Joint UK DECC/Defra Met Office Hadley Centre  
416 Climate Programme (GA01101) and by the NERC Changing Water Cycle (South Asia) project  
417 SAPRISE, grant number NE/I022469/1.

418

419

420 **References**

- 421 Adler, R.F., G.J. Huffman, A. Chang, R. Ferraro, P. Xie, J. Janowiak, B. Rudolf, U. Schneider,  
422 S. Curtis, D. Bolvin, A. Gruber, J. Susskind, P. Arkin, E. Nelkin: The Version 2 Global  
423 Precipitation Climatology Project (GPCP) Monthly Precipitation Analysis (1979-Present). *J.*  
424 *Hydrometeor.*, 4, 1147-1167, 2003.
- 425 Baek, H.-J., J. Lee, H.-S. Lee, C. Cho, W.-T. Kwon, C. Marzin, Y.-K. Hyun, S.-Y. Gan, M.-J.  
426 Kim, D.-H. Choi, J. Lee, J. Lee, K.-O. Boo, H.-S. Kang, and Y.-H. Byun: Climate change in  
427 the 21<sup>st</sup> century simulated by HadGEM2-AO under Representative Concentration Pathways,  
428 *Asia-Pac. J. Atmos. Sci.*, 49(5), 603-618, 2013.
- 429 Bayer, L. B., B. J. J. M. van den Hurk, B. J. Strengers, and J. G. van Minnen: Regional  
430 feedbacks under changing climate and land-use conditions, *Earth Syst. Dynam. Discussions*, 3,  
431 201–234, doi:10.5194/esdd-3-201-2012, 2012.
- 432 Cox, P. M., R. A. Betts, C. B. Bunton, R. L. H. Essery, P. R. Rowntree, and J. Smith: The  
433 impact of new land surface physics on the GCM simulation of climate and climate sensitivity,  
434 *Clim. Dynam.*, 15, 3, 183–203, doi:10.1007/s003820050276, 1999.
- 435 Cox, P. M.: Description of the “TRIFFID” Dynamic Global Vegetation Model, Hadley Centre  
436 Technical Note No. 24, available from: [http://www.metoffice.gov.](http://www.metoffice.gov.uk/learning/library/publications/science/climate-science/hadley-centre-technical-note)  
437 [uk/learning/library/publications/science/climate-science/hadley-centre-technical-note](http://www.metoffice.gov.uk/learning/library/publications/science/climate-science/hadley-centre-technical-note), last  
438 access: 20 July 2012, Met Office Hadley Centre, Exeter, UK, 2001.
- 439 Collins, W. J., Bellouin, N., Doutriaux-Boucher, M., Gedney, N., Halloran, P., Hinton, T.,  
440 Hughes, J., Jones, C. D., Joshi, M., Liddicoat, S., Martin, G., O’Connor, F., Rae, J., Senior, C.,  
441 Sitch, S., Totterdell, I., Wiltshire, A., and Woodward, S.: Development and evaluation of an  
442 Earth-System model – HadGEM2, *Geosci. Model Dev.*, 4, 1051–1075, doi:10.5194/gmd-4-  
443 1051-2011, 2011.
- 444 Douglas, E. M., D. Niyogi, S. Frohking, J. B. Yeluripati, R. A. Pielke Sr., N. Niyogi, C. J.  
445 Vorosmarty, and U. C. Mohanty: Changes in moisture and energy fluxes due to agricultural



446 land use and irrigation in the Indian Monsoon Belt, *Geophys. Res. Lett.*, 33, L14403,  
447 doi:10.1029/2006GL026550, 2006.

448 Essery, R. and D. B. Clark: Developments in the MOSES 2 land-surface model for PILPS 2e,  
449 *Global Planet. Change*, 38, 161–164, doi:10.1016/j.bbr.2011.03.031, 2003.

450 Harris, I., Jones, P.D., Osborn, T.J., and Lister, D.H.: Updated high-resolution grids of monthly  
451 climatic observations – the CRU TS3.10 Dataset, *Int. J. Climatol.*, 34, 623-642, Doi:  
452 10.1002/joc.3711, 2013.

453 Huffman, G.J, R.F. Adler, D.T. Bolvin, G. Gu: Improving the Global Precipitation Record:  
454 GPCP Version 2.1, *Geophys. Res. Lett.*, 36, L17808, doi:10.1029/2009GL040000, 2009.

455 Hurrell, J., Meehl, G. A., Bader, D., Delworth, T. L., Kirtman, B., and Wielicki, B.: A unified  
456 modeling approach to climate system prediction, *B. Am. Meteorol. Soc.*, 90, 1819–1832,  
457 doi:10.1175/2009BAMS2752.1, 2009.

458 Hurtt, G. C., Chini, L. P., Frohking, S., Betts, R., Feddema, J., Fischer, G., Fisk, J. P., Hibbard,  
459 K., Houghton, R. A., Janetos, A., Jones, C., Kindermann, G., Kinoshita, T., Klein Goldewijk,  
460 K., Riahi, K., Shevliakova, E., Smith, S., Stehfest, E., Thomson, A., Thornton, P., van Vuuren,  
461 D. P., and Wang, Y.: Harmonization of Land-Use Scenarios for the Period 1500–2100: 600  
462 Years of Global Gridded Annual Land-Use Transitions, Wood Harvest, and Resulting  
463 Secondary Lands, *Climatic Change*, 109, 117–161, doi:10.1007/s10584-011-0153-2, 2011.

464 Jones, C. D., Hughes, J. K., Bellouin, N., Hardiman, S. C., Jones, G. S., Knight, J., Liddicoat,  
465 S., O’Connor, F. M., Andres, R. J., Bell, C., Boo, K.-O., Bozzo, A., Butchart, N., Cadule, P.,  
466 Corbin, K. D., Doutriaux-Boucher, M., Friedlingstein, P., Gornall, J., Gray, L., Halloran, P. R.,  
467 Hurtt, G., Ingram, W. J., Lamarque, J.-F., Law, R. M., Meinshausen, M., Osprey, S., Palin, E.  
468 J., Parsons Chini, L., Raddatz, T., Sanderson, M. G., Sellar, A. A., Schurer, A., Valdes, P.,  
469 Wood, N., Woodward, S., Yoshioka, M., and Zerroukat, M.: The HadGEM2-ES  
470 implementation of CMIP5 centennial simulations, *Geosci. Model Dev.*, 4, 543–570,  
471 doi:10.5194/gmd-4-543-2011, 2011.

472 Kang, H.-S., D.-H. Cha and D.-K. Lee: Evaluation of the mesoscale model/land surface model  
473 (MM5/LSM) coupled model for East Asian summer monsoon simulations, *J. Geophys. Res.*,  
474 110, D10105, doi:10.1029/2004JD005266, 2005.

475 Kang, H.-S. and S.-Y. Hong: An assessment of the land surface parameters on the simulated  
476 regional climate circulations: The 1997 and 1998 east Asian summer monsoon cases, *J.*  
477 *Geophys. Res.*, 113, D15121, doi:10.1029/2007D009499, 2008.

478 Konaré, A., A. S. Zakey, F. Solmon, F. Giorgi, S. Rauscher, S. Ibrah, and X. Bi: A regional  
479 climate modeling study of the effect of desert dust on the West African monsoon, *J. Geophys.*  
480 *Res.*, 113, D12206, doi:10.1029/2007JD009322, 2008.

481 Lau, K. M., M.-T. Li: The monsoon of East Asia and its global associations-A survey, *B. Am.*  
482 *Meteorol. Soc.*, 65, 114-125, 1984.

483 Lau, K. M., M. K. Kim, and K. M. Kim: Asian monsoon anomalies induced by aerosol direct  
484 effects, *Clim. Dyn.*, 26, 855– 864, doi:10.1007/s00382-006-0114-z, 2006.

485 Lau, K. M and K.-M. Kim: Observational relationships between aerosol and Asian monsoon  
486 rainfall, and circulation, *Geophys. Res. Lett.*, 33, L21810, doi:10.1029/2006GL027546, 2006.

487 Lawrence. D. M. and J. M. Slingo: An annual cycle of vegetation in a GCM. Part I:  
488 implementation and impact on evaporation, *Clim. Dynam.*, 22, 87–105, doi:10.1007/s00382-  
489 003-0366-9, 2004.

490 Lee, E., T. N. Chase, B. Rajagopalan, R. G. Barry, T. W. Biggs, and P. J. Lawrence: Effects of  
491 irrigation and vegetation activity on early Indian summer and monsoon variability, *Int. J.*  
492 *Climatol.*, 29, 573–581, doi:10.1002/joc.1721, 2009.

493 Lee, E., C. C. Barford, C. J. Kucharik, B. S. Felzer, and J. A. Foley: Role of turbulent heat  
494 fluxes over land in the monsoon over East Asia, *Int. J. Geosci.*, 2, 420–431,  
495 doi:10.4236/ijg.2011.24046, 2011.

496 Lee, E. J., S. W. Yeh, J. G. Jhun and B. K. Moon: Seasonal change in anomalous WNPSH  
497 associated with the strong East Asian summer monsoon, *Geo. Res. Let.*, 33, L21702, 2006.

498 Loveland, T. R., B. C. Reed, J. F. Brown, D. O. Ohlen, Z. Zhu, L. Yang, and J. W. Merchant:  
499 Development of a global land cover characteristics database and IGBP DISCover from 1 km  
500 AVHRR data, *Int. J. Remote Sensing*, 21, 1303–1330, doi:10.1080/014311600210191, 2000.

501 Martin, G. M. and R.C. Levine: The influence of dynamic vegetation on the present-day  
502 simulation and future projections of the South Asian summer monsoon in the HadGEM2 family,  
503 *Earth Syst. Dynam.*, 3, 245-261, doi:10.5194/esd-3-245-2012, 2012.

504 McCarthy, M. P., Sanjay, J., Booth, B. B. B., Krishna Kumar, K., and Betts, R. A.: The  
505 influence of vegetation on the ITCZ and South Asian monsoon in HadCM3, *Earth Syst.*  
506 *Dynam.*, 3, 87–96, doi:10.5194/esd-3-87-2012, 2012.

507 Miller, R. L., and I. Tegen: Climate response to soil dust aerosols, *J. Clim.*, 11, 3247–3267,  
508 1998.

509 Paeth, H., and J. Feichter: Greenhouse-gas versus aerosol forcing and African climate response,  
510 *Clim. Dyn.*, 26, 35– 54, 2005.

511 Qian Y, D. Gong, J. Fan, L. R. Leung, R. Bennartz, D. Chen and W. Wang: Heavy pollution  
512 suppresses light rain in China: Observations and modeling, *J. Geophys. Res.*, 114, D00K02,  
513 doi:10.1029/2008JD011575, 2009.

514 Ramanathan, V., C. Chung, D. Kim, T. Betge, L. Buja, J. T. Kiehl, W. M. Washington, Q. Fu,  
515 D. R. Sikka, and M. Wild: Atmospheric brown clouds: Impacts on South Asian climate and  
516 hydrological cycle, *Proc. Natl. Acad. Sci. U. S. A.*, 102, 5326 – 5333,  
517 doi:10.1073/pnas.0500656102, 2005.

518 Seo K.-H, O. Ok J., J.-H. Son, D.-H. Cha: Assessing future changes in the East Asian summer  
519 monsoon using CMIP5 coupled Models, *J. Clim.*, 26, 7662-7675, DOI: 10.1175/JCLI-D-12-  
520 00694.1, 2013.

521 Sokolik I. N. and O. B. Toon: Direct radiative forcing by anthropogenic airborne mineral  
522 aerosols, *Nature*, 381, 681-683, 1996.

523 Suh M.-S. and D.-K. Lee: Impacts of land use/cover changes on surface climate over east Asia  
524 for extreme climate cases using RegCM2, *J. Geophys. Res.*, 109, D02108,  
525 doi:10.1029/2003JD003681, 2004.

526 Taylor, K. E., Stouffer, R. J., and Meehl, G. A: An Overview of CMIP5 and the experiment  
527 design, *B. Am. Meteorol. Soc.*, 93, 485–498, doi:10.1175/BAMS-D-11-00094.1, 2012.

528 The HadGEM2 Development Team: Martin, G. M., Bellouin, N., Collins, W. J., Culverwell, I.  
529 D., Halloran, P. R., Hardiman, S. C., Hinton, T. J., Jones, C. D., McDonald, R. E., McLaren,  
530 A. J., O'Connor, F. M., Roberts, M. J., Rodriguez, J. M., Woodward, S., Best, M. J., Brooks,  
531 M. E., Brown, A. R., Butchart, N., Dearden, C., Derbyshire, S. H., Dharssi, I., Doutriaux-  
532 Boucher, M., Edwards, J. M., Falloon, P. D., Gedney, N., Gray, L. J., Hewitt, H. T., Hobson,  
533 M., Huddleston, M. R., Hughes, J., Ineson, S., Ingram, W. J., James, P. M., Johns, T. C.,  
534 Johnson, C. E., Jones, A., Jones, C. P., Joshi, M. M., Keen, A. B., Liddicoat, S., Lock, A. P.,  
535 Maidens, A. V., Manners, J. C., Milton, S. F., Rae, J. G. L., Ridley, J. K., Sellar, A., Senior, C.  
536 A., Totterdell, I. J., Verhoef, A., Vidale, P. L., and Wiltshire, A: The HadGEM2 family of Met  
537 Office Unified Model climate configurations, *Geosci. Model Dev.*, 4, 723-757,  
538 doi:10.5194/gmd-4-723-2011, 2011.

539 Webster, P. J., Magana V. O., Palmer T. N., Shukla J., Tomas R. A., Yanai M. and Yasunari  
540 T.: Monsoons: Processes, Predictability, and the Prospects for Prediction, *Journal of*  
541 *Geophysical Research*, 3, 14451-14510. doi:10.1029/97JC02719, 1998.

542 Woodward, S.: Mineral dust in HadGEM2. Hadley Centre Technical Note 87, Met Office  
543 Hadley Centre., Exeter, EX1 3PB, UK, available from  
544 <http://www.metoffice.gov.uk/learning/library/publications/science/climate-science-technical->  
545 notes (last access: 18 December 2014), 2011.

546 Xie, P., and P. A. Arkin: Global precipitation: A 17-year monthly analysis based on gauge  
547 observations, satellite estimates, and numerical model outputs. *Bull. Amer. Meteor. Soc.*, 78,  
548 2539 – 2558, 1997.

549 Yamashima, R., K. Takata, J. Matsumoto, and T. Yasunari: Numerical study of the impacts of  
550 land use/cover changes between 1700 and 1850 on the seasonal hydroclimate in monsoon Asia,  
551 J. Meteorol. Soc. Japan, 89A, 291–298, doi:10.2151/jmsj.2011-A19, 2011.

552 Yoshioka, M., N. M. Mahowald, A. J. Conley, W. D. Collins, D. W. Fillmore, C. S. Zender  
553 and D. B. Coleman: Impact of desert dust radiative forcing on Sahel precipitation: relative  
554 importance of dust compared to sea surface temperature variations, vegetation changes, and  
555 greenhouse gas warming, J. Clim., 20, 1445-1467, DOI: 10.1175/JCLI4056.1, 2007.

556 Table 1. List of experiments.

557

Acronym	Description of the experiments	Time
A	HadGEM2-A	
AE	HadGEM2-A with ES vegetation	Present
Anod	HadGEM2-A with no dust radiative effects	1980-2005
AEnod	HadGEM2-A with ES vegetation with no dust radiative effects	
Ats	HadGEM2-A time slice run	
AEts	HadGEM2-A with ES vegetation time slice run	Future
AEnodts	HadGEM2-A with ES vegetation time slice run with no dust radiative effects	2080-2110

558

559 Table 2. Impacts of climate change of global warming, land cover change and dust loading  
 560 obtained by the difference between the experiments in this study.

Impact	Descriptions
Climate change (Global warming)	$A_{ts} - A$
Climate change + LCC + Dust	$A_{Ets} - AE$
Climate change + LCC	$A_{Enodts} - A_{Enod}$
Dust	$(A_{Ets} - AE) - (A_{Enodts} - A_{Enod})$
LCC (ES land cover)	$(A_{Enodts} - A_{Enod}) - (A_{ts} - A)$

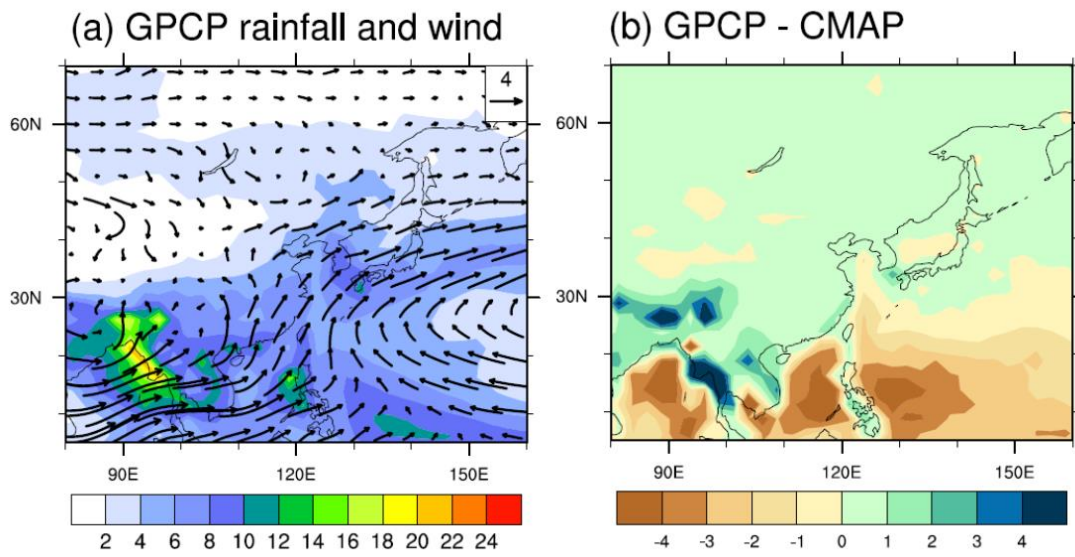
561

562

563

564

565



566

567

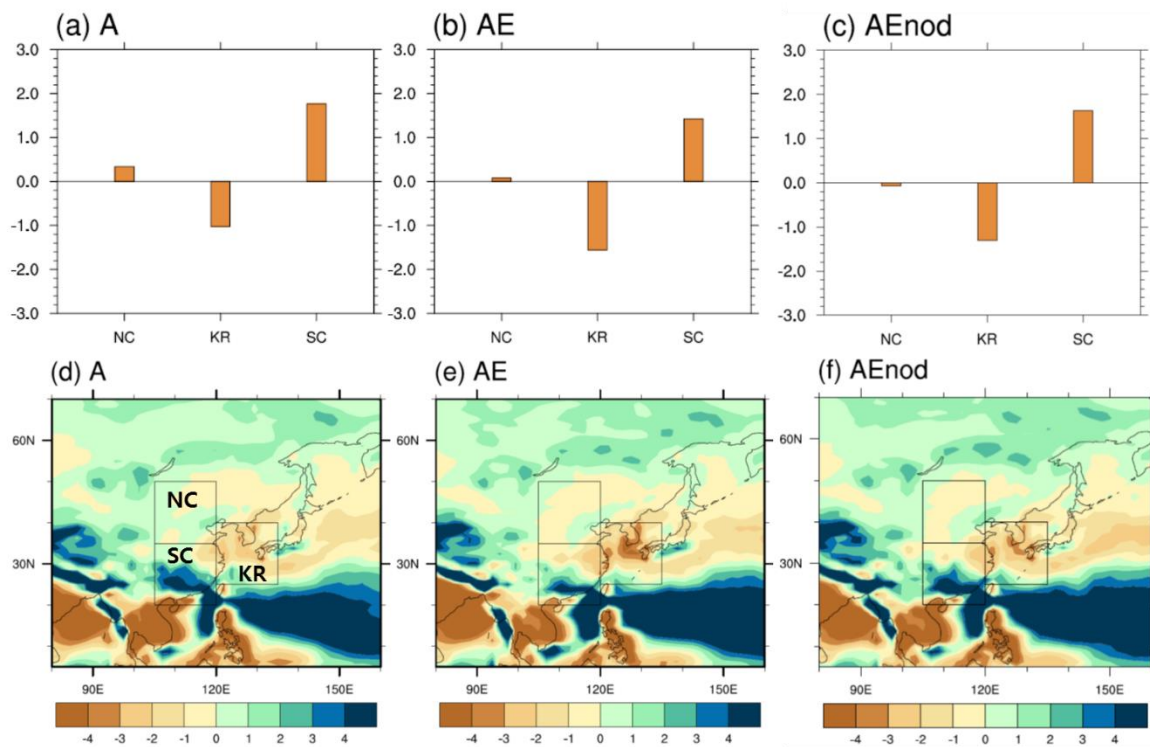
568 Figure 1. The 1982-2005 JJA (a) climatology of the Global Precipitation Climatology Project  
 569 (GPCP) precipitation ( $\text{mm day}^{-1}$ , shading) and 850hPa winds ( $\text{m s}^{-1}$ ) and (b) precipitation  
 570 difference between GPCP and the CPC Merged Analysis of Precipitation (CMAP)

571



572

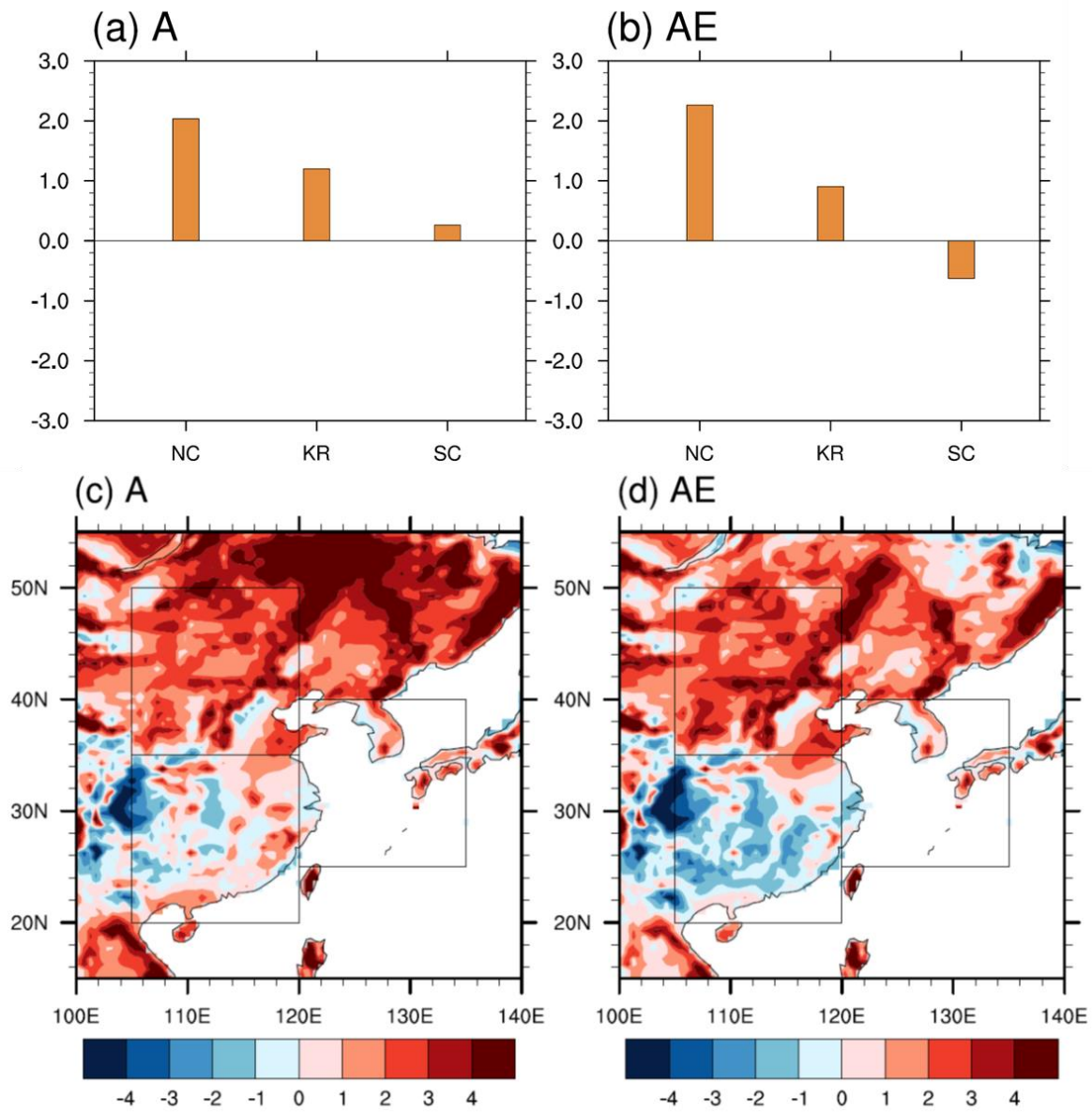
573



574

575 Figure 2. Area averaged JJA precipitation bias ( $\text{mm day}^{-1}$ ) compared to the Global  
576 Precipitation Climatology Project (GPCP) observation: (a, b and c) show regional mean  
577 biases over the regions shown in (d, e and f). NC region:  $35\text{-}50^\circ\text{ N}$ ,  $105\text{-}120^\circ\text{ E}$ ; KR:  $25\text{-}40^\circ$   
578  $\text{N}$ ,  $120\text{-}135^\circ\text{ E}$ ; SC region:  $20\text{-}35^\circ\text{ N}$ ,  $105\text{-}120^\circ\text{ E}$ .

579



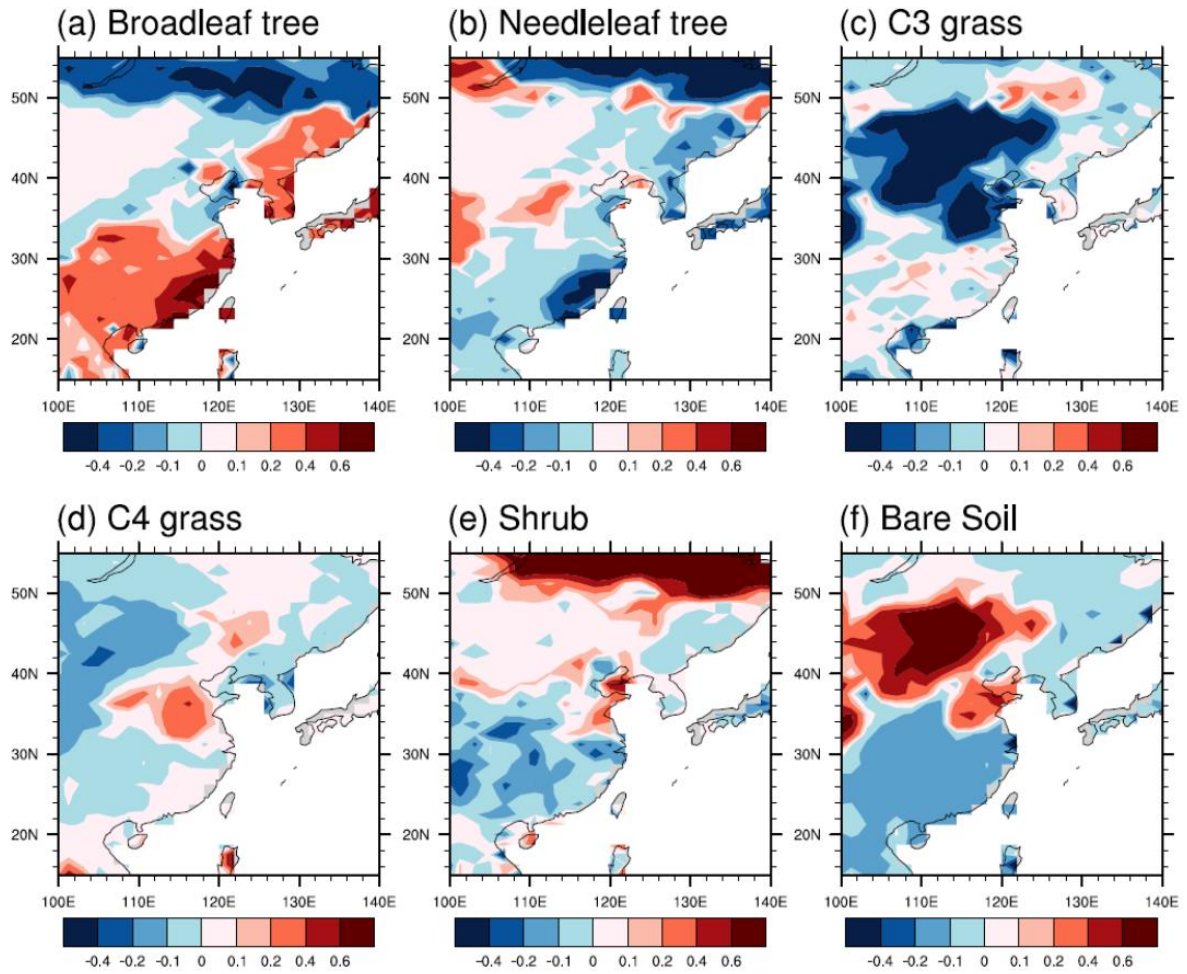
580

581

582 Figure 3. As Fig. 1 but for JJA surface air temperature biases (K) compared to the Climatic  
 583 Research Unit (CRU) climatology.

584

585



586

587

588 Figure 4. Differences in present-day (1980-2005) fractions of land cover type between  
 589 HadGEM2-ES and HadGEM2-AO (and HadGEM2-A) over East Asia.

590

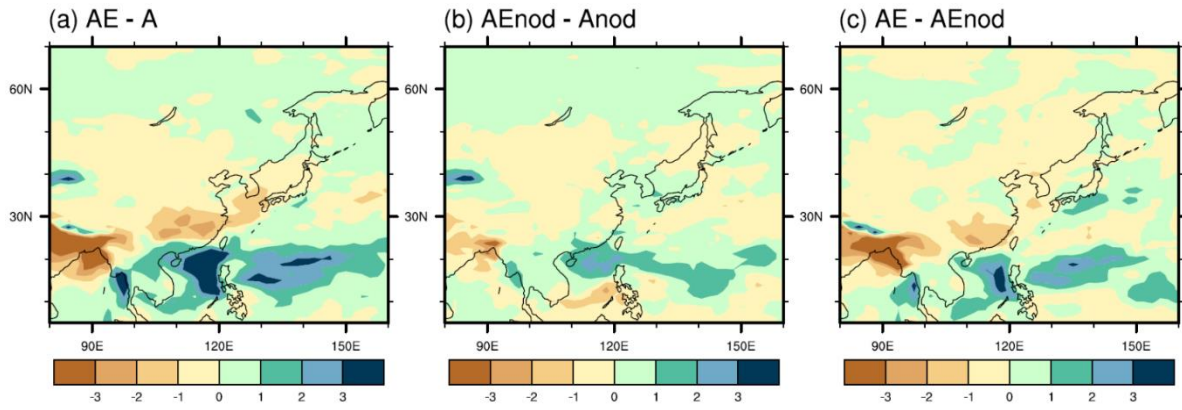
591

592

593

594

595



596

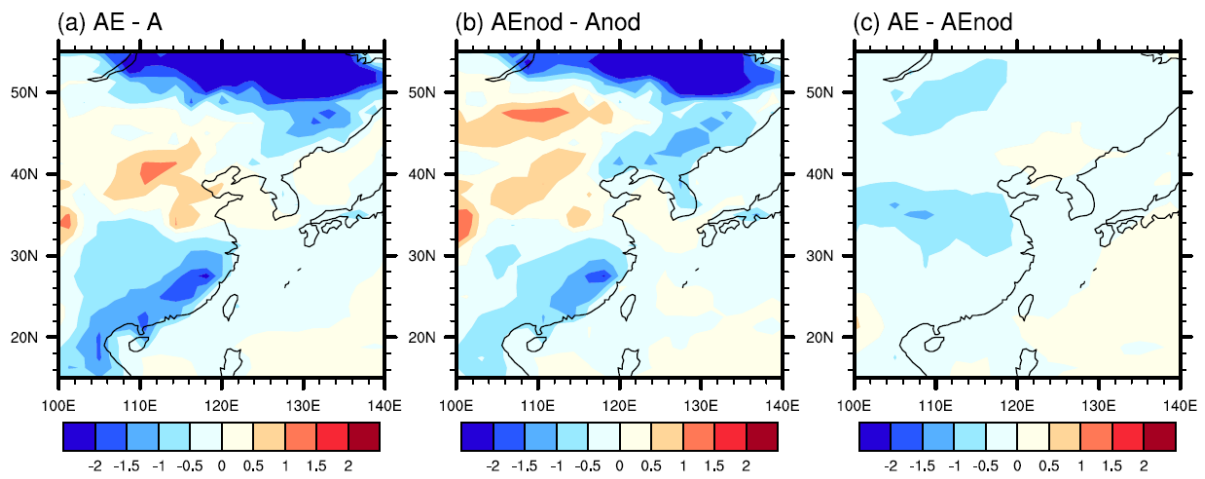
597

598 Figure 5. Precipitation differences ( $\text{mm day}^{-1}$ ) in JJA for (a) AE minus A (b) AEnod minus  
 599 Anod, and (c) AE minus AEnod.

600

601

602



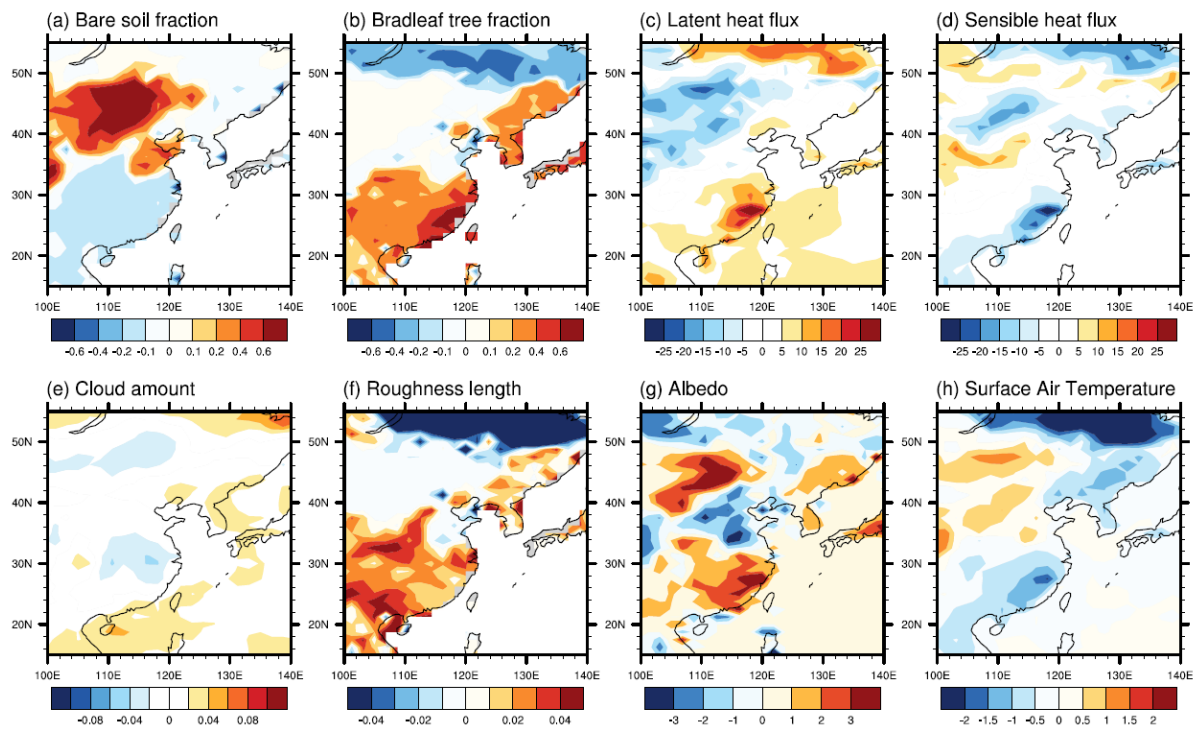
603

604

605 Figure 6. Surface air temperature differences (K) in JJA for (a) AE minus A, (b) AEnod  
 606 minus Anod, (c) AE minus AEnod.

607

608

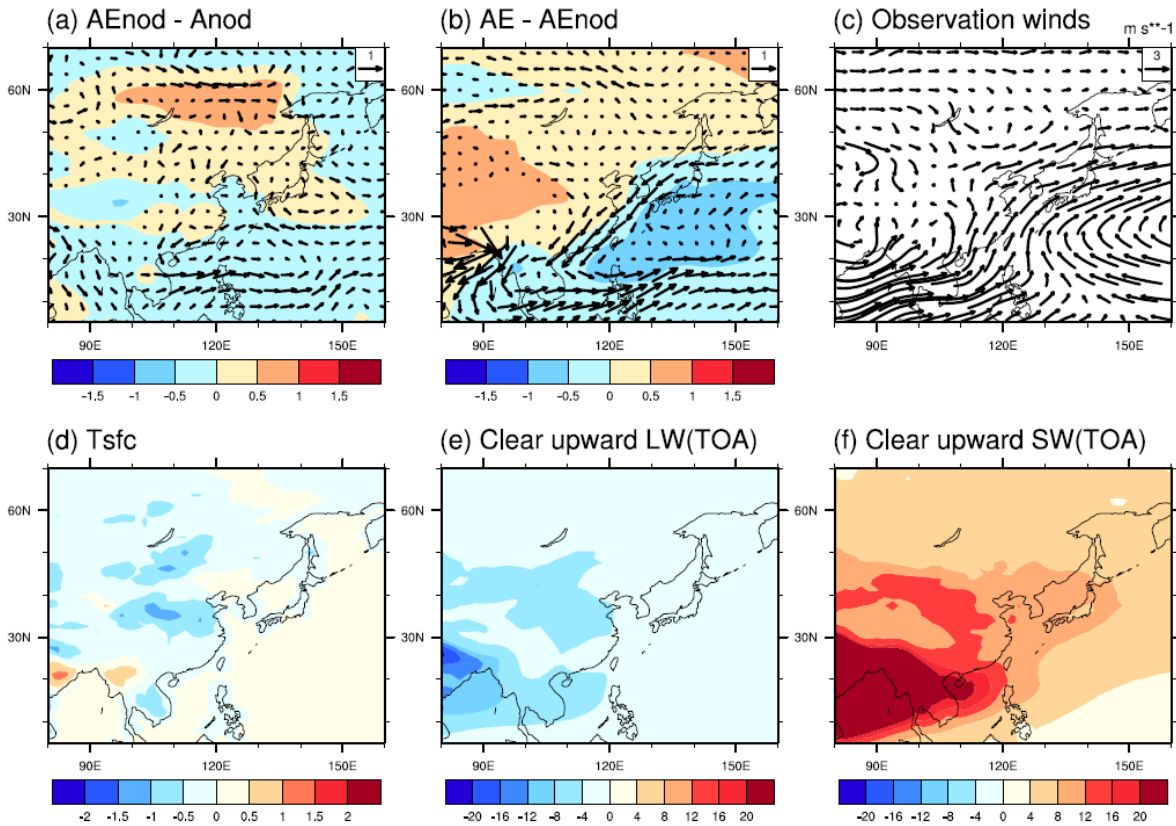


609

610 Figure 7. AEnod minus Anod in JJA showing the applied fractional land cover changes and  
 611 their impact in (a) bare soil fraction, (b) broadleaf tree fraction, (c) latent heat flux ( $\text{W m}^{-2}$ ), (d)  
 612 sensible heat flux ( $\text{W m}^{-2}$ ), (e) cloud amount (fraction), (f) roughness length (m), (g) albedo  
 613 (%) and (h) surface air temperature (K).

614

615



616

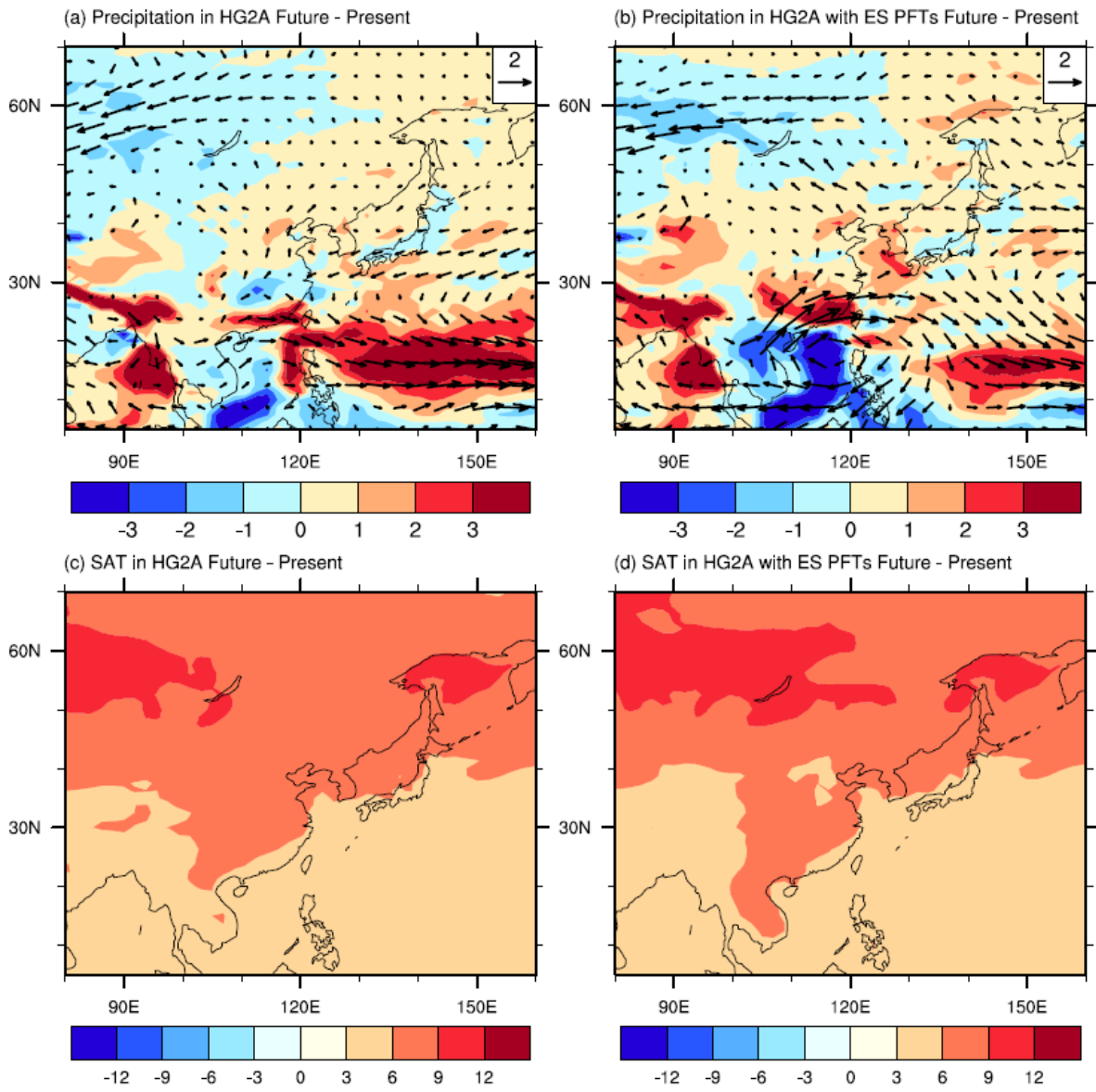
617

618 Figure 8. Changes in mean sea level pressure (hPa) and 850 hPa winds ( $\text{m s}^{-1}$ ) in JJA for (a)  
619 AEnod minus Anod, and (b) AE minus AEnod. (c) Climatology of 850 hPa winds for the period  
620 1982-2005 using ERA Interim; (d to f) show differences between AE and AEnod in JJA: (d)  
621 surface temperature (K), (e) clear sky upward longwave radiation ( $\text{W m}^{-2}$ ) and (f) clear sky  
622 upward shortwave radiation ( $\text{W m}^{-2}$ ) at top of atmosphere, showing the impacts of the radiative  
623 effects from additional dust loading induced by the ES land cover.

624

625

626



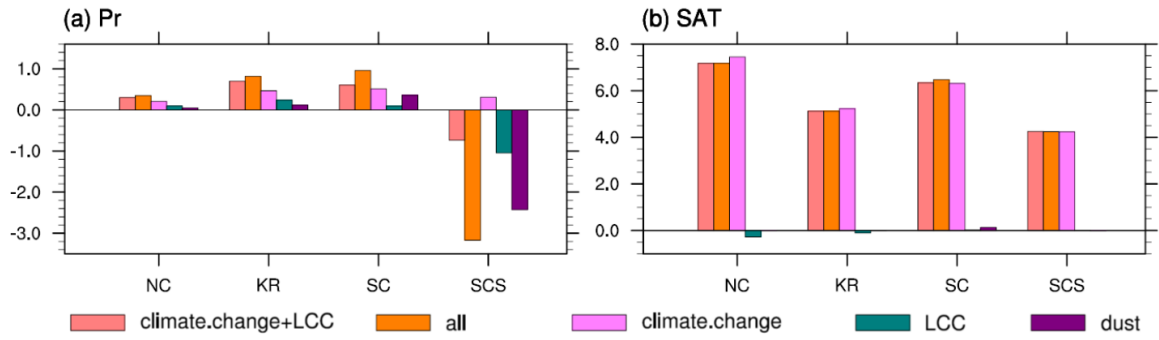
628

629

630 Figure 9. Changes in JJA mean precipitation (shading,  $\text{mm day}^{-1}$ ) between future timeslice and  
631 present-day HadGEM2-A experiments, without (a, c) and with (b, d) land cover from  
632 HadGEM2-ES. (a), (c) is (Ats-A) and (b), (d) is (AEts-AE).

633



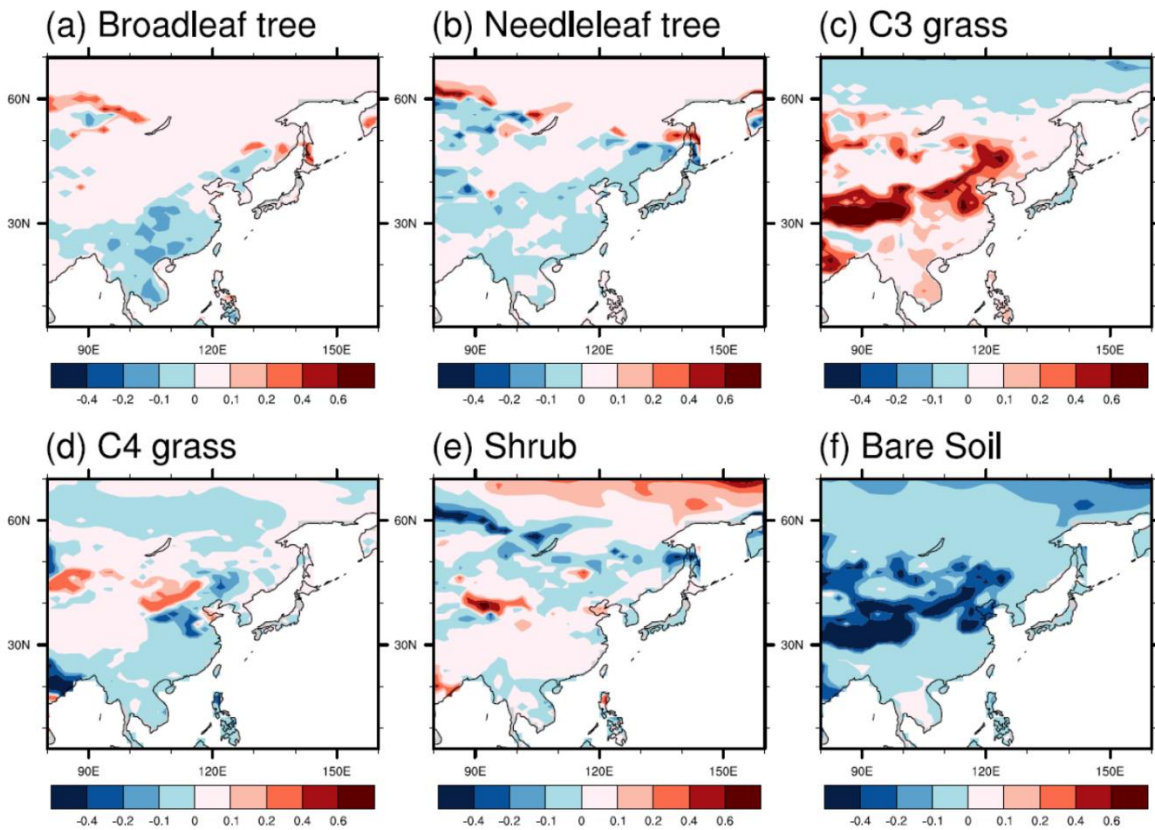


634

635 Figure 10. Future changes of precipitation (mm day<sup>-1</sup>) (a) and surface air temperature (K) (b)  
 636 over the box regions of North China (NC), Korea (KR), South China (SC) and South China  
 637 Sea (SCS) in summer. Note that “all” means sum of climate change, land cover change and  
 638 direct radiative effect of dust; “LCC” and “Dust” are ‘double-differences’ illustrating the  
 639 influence of those processes on the future-present changes.

640

641

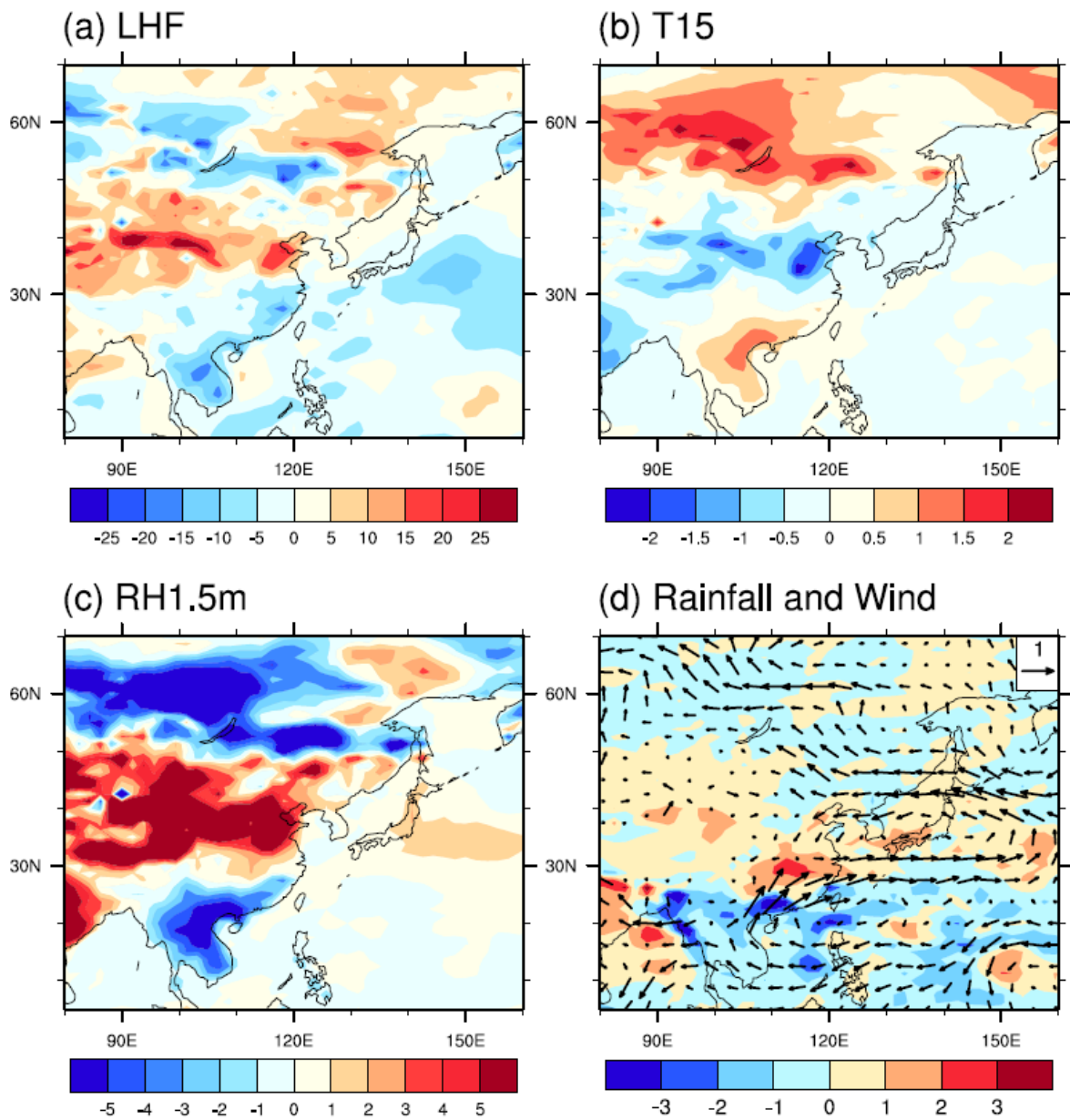


642

643

644 Figure 11. Changes of fractions in land cover between c.2100 and present-day as simulated by  
 645 HadGEM2-ES in the Fifth Coupled Model Intercomparison Project (CMIP5) the  
 646 Representative Concentration Pathway (RCP) 8.5 scenario and applied in AE present and AETs  
 647 future time-slice experiments.

648

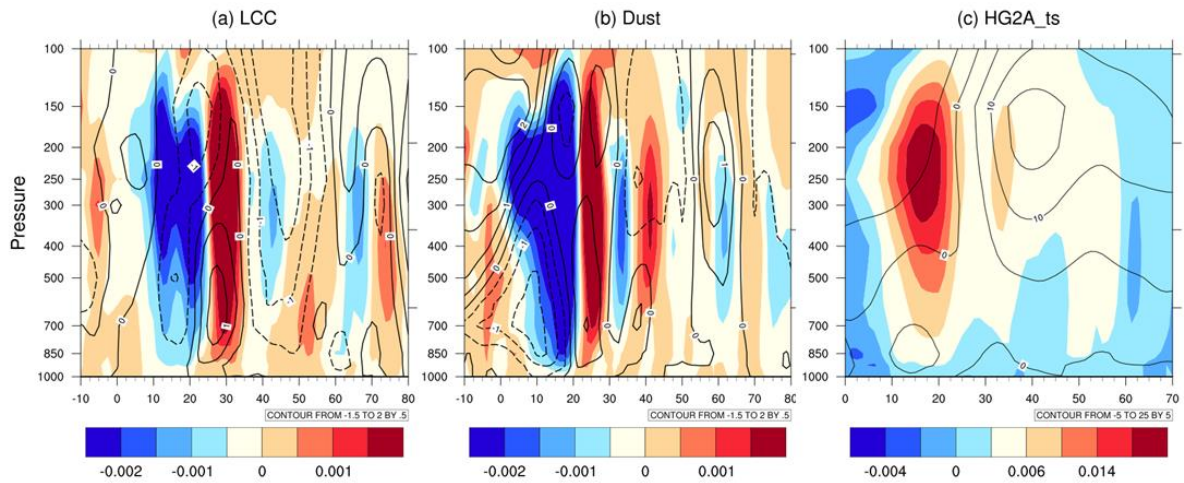


649

650

651 Figure 12. Contribution by the land cover changes alone to the future-present differences in  
 652 JJA (represented by  $(AEnodts - AEnod) - (Ats - A)$ ) in (a) latent heat flux ( $W m^{-2}$ ), (b) surface  
 653 air temperature (K), (c) 1.5 m relative humidity (%) and (d) rainfall (shading,  $mm day^{-1}$ ), 850  
 654 hPa wind (vectors,  $m s^{-1}$ ).

655

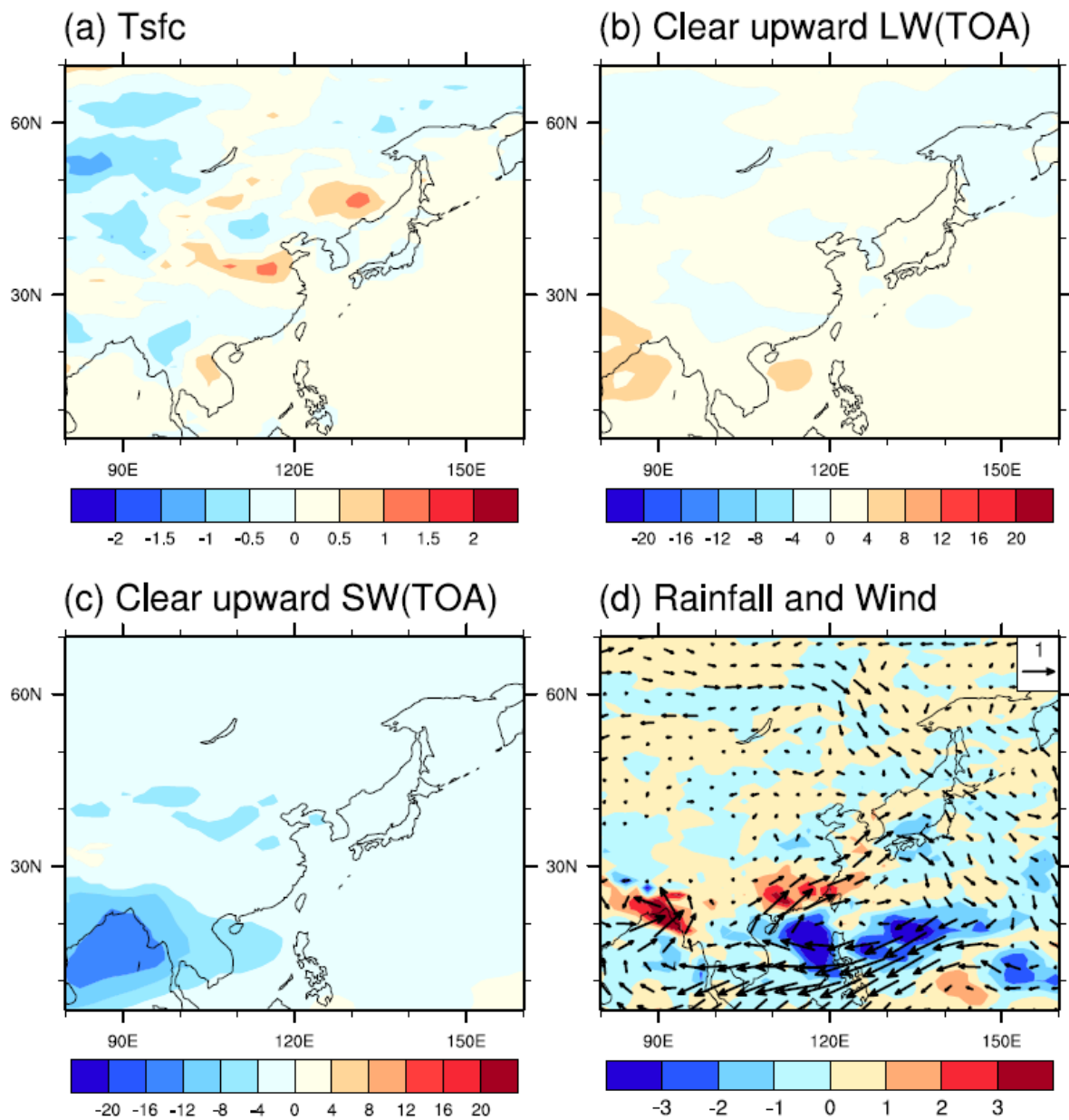


656

657

658 Figure 13. (a and b) Contribution to future-present changes in vertical motion (upward: red,  
 659 downward: blue) and U wind anomalies (solid line: westerlies) from 110-120° E driven by  
 660 (a) LCC impact, and (b) dust impact. (c) Climatological vertical motion over 110-120° E in  
 661 the HadGEM2-A timeslice run, Ats.

662

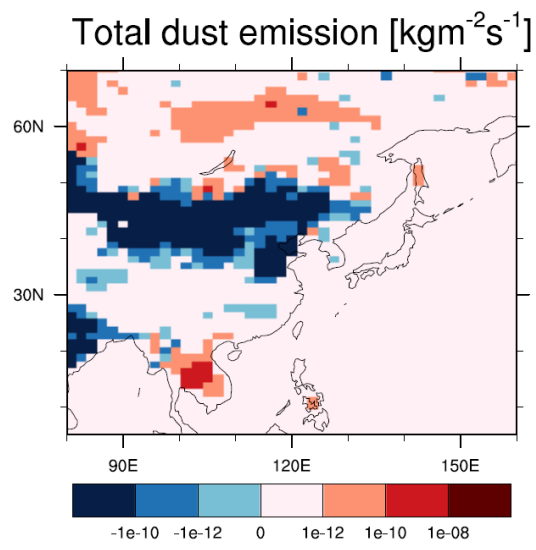


663

664

665 Figure 14. As Fig. 13 but showing the contribution from the direct radiative effect of dust to  
 666 the future-present differences (represented by  $(AE_{ts} - AE) - (AE_{nodts} - AE_{nod})$ ) in JJA in  
 667 (a) surface temperature (K), (b) clear sky upward longwave radiation at top of atmosphere ( $W m^{-2}$ ), (c)  
 668 clear sky upward shortwave radiation at top of atmosphere ( $W m^{-2}$ ) and (d) rainfall  
 669 (shading,  $mm day^{-1}$ ), 850 hPa wind (vectors,  $m s^{-1}$ ).

670



671

672

673 Figure 15. Future changes in total dust emission ( $\text{kg m}^{-2} \text{s}^{-1}$ ) in JJA from AETs – AE.

674